Journal of Inclusion Phenomena and Macrocyclic Chemistry **39:** 261–267, 2001.

Complexes of Rare Earths and Dipicolinato Ions Encapsulated in X- and Y-zeolites: Luminescence Properties

JEANNETTE DEXPERT-GHYS[1,*], CLAUDE PICARD[2] and AGNES TAURINES[1]
[1]*CEMES/CNRS, 29 rue J. Marvig, BP 4347, 31055 Toulouse Cedex 4, France;* [2]*LSPCMIB, UMR 5068 CNRS, Université Paul Sabatier, 118 route de Narbonne, 31062 Toulouse Cedex 4, France*

(Received: 24 March 2000; in final form: 25 August 2000)

Key words: rare earth, lanthanide, zeolite, host-guest, luminescence.

Abstract

The complexes {Ln(DP)}Z where Ln^{3+} = La^{3+} or Eu^{3+}, DP is the dipicolinate ion (2,6)-pyridine dicarboxylate: $C_5H_3N(COO^-)_2$ and Z = one of the faujasite-type X or Y zeolites have been synthesized and investigated by XRD, Raman and IR spectroscopy, and Eu^{3+} luminescence spectroscopy. The rare earth complexes are synthesized inside the super-cages of the zeolites; the degree of complexation never exceeds 1DP/1Ln. Only the Ln ions, which are in the super-cages, may be complexed. Luminescent europium complexes encapsulated in zeolite matrices were obtained. The $^5D_0 \rightarrow F_J$ luminescence observed under excitation into the lowest-energy ligand-centered absorption band (275 nm) indicates that a DP to Eu energy transfer occurs in these systems. The complex versus the zeolite framework conformations influence the europium emission characteristics: the transfer is more efficient when the complexed europium $[Eu(DP)]^+$ is directly bonded to the framework oxygen atoms rather than to a residual water molecule.

Introduction

Many syntheses of transition metal complexes encapsulated within the cages of a zeolite framework (usually the commercial faujasite type Y-zeolite) have been performed in the last decades. The resulting complexes, designated as {M(L)}Z have been investigated in relation to their potential applications. Among numerous studies, one may mention for instance: zeolite encapsulated metal porphyrins and metal phthalocyanines used as biomimetic catalysts [1–3], electrocatalysis by encapsulated Co(salen) and $[Fe(bpy)_3]^{2+}$ (salen = *N*, *N*′-bis-(salicylidene)ethylenediamine and bpy = 2,2′-bipyridine) [4], photocatalytic processes in encapsulated [RuIII(bpy)1] [5]. Another route followed in Ref. [6] is the synthesis of zeolite polytypes templated by a Gd(III) complex of 18-crown-6 (1,4,7,10,13,16-hexaoxacyclo-octadecane), the templating agent stays encapsulated in the zeolite at the end of the synthesis. These materials have potential applications in magnetic resonance imaging.

In the field of rare earth containing luminescent materials, several attempts to synthesize organic-inorganic hybrids have also been successful. Rare earth chelates have been introduced by sol-gel methods in silicate matrices, either by simple mixing of the chelate with a silicate precursor [7], or by covalently bonding the complexing agent to the silicate precursor prior to complexation and sol-gel processing [8]. On the other hand, $[Eu(bpy)_2]^{3+}$ supported on zeolite Y has been studied by luminescence [9], the authors conclude that zeolites are efficient host lattices for the rare earth bonded to an appropriate ligand as an antenna. Recently Alvaro et al. [10] reported on the characterization of highly luminescent europium complexes, including those with the dipicolinate ligand, inside zeolites Y and mordenite. The same kind of luminescent Eu^{3+} and Tb^{3+} complexes in zeolite X was also investigated by Hilder et al. [11].

This paper deals with the complexes: {Ln(DP)}Z where Ln^{3+} = La^{3+} or Eu^{3+}, L = DP for the dipicolinate (2,6-pyridine dicarboxylate) ion

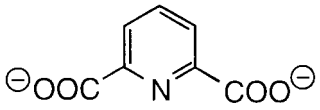

and Z = one of the faujasite-type X or Y zeolites. One aim of this work is to analyze the potential luminescence properties of the europium-doped hybrids. On the other hand, some structural aspects of these materials were determined using the results of X-ray diffraction, optical, IR and Raman spectroscopies. For this last purpose, the lanthanum-doped hybrids were also considered. Systems that could serve as references for the (Eu–DP) pair were also investigated: the complexes [1Eu–3DP] in aqueous solution and $[Eu(DP)_3Na_3]\cdot nH_2O$ in the solid state.

* Author for correspondence.

Experimental

Sample preparations and analysis

NaY and NaX zeolites were purchased from Union Carbide. Lanthanum and europium nitrates (99.99%) were kindly given by Rhodia. DPH_2 (2,6-pyridine dicarboxylic acid) was purchased from Aldrich.

The cation exchange was carried out in a closed vessel under pseudo-hydrothermal conditions at 120 °C during 2.5 days. 1 g of the zeolite was immersed in 12 mL of a rare earth nitrate aqueous solution (pH = 5 ± 0.5). The initial Ln concentration was adjusted to a $2Ln^{3+}/3Na^{+}$ ratio, with $[Na^{+}]$ given in the theoretical formulas. After reaction, the vessel was cooled down slowly. The powder was filtered and carefully washed with water, then dried at room temperature. Parts of the Eu-exchanged powders were submitted to calcination under a nitrogen flux successively for 9 h at 100 °C, 2 h at 200 °C and 2 h at 400 °C. The samples were slowly cooled down then kept under the laboratory atmosphere, thus allowed re-hydration. They are denoted as {EU}YC and {EU}XC.

The complexation by the ligand DP = $C_5H_3N(COO^{-})_2$ was carried out under the same experimental conditions as those described for the exchange. To 0.5 g of {Ln}X, {Ln}Y (about 0.025 mmol), or of the calcined equivalents, was added 0.54 mmol of DPH_2 in ethanol (12 mL). After treatment in a closed vessel at 120 °C for 2.5 days, the resulting powder was filtered, washed several times with ethanol, then dried at room temperature.

$[Eu(DP)_3Na_3]\cdot nH_2O$ was prepared following a described procedure [12]

1Eu–3DP aqueous solution was prepared by dissolving $Eu(NO_3)_3\cdot 6H_2O$ (0.1 mmol) and DPH_2 (0.3 mmol) in 20 mL of water. The pH was adjusted to ∼ 7 with diluted NaOH. The 1Eu–3DP mother solution was then diluted in water up to 4×10^{-5} M.

Investigation techniques

The elemental analyses were carried out by the "Service Central d'Analyses du CNRS" in Vernaison (France).

The powder X-ray diffraction patterns were recorded on a Seifert MZ6 apparatus (θ/θ). The IR spectra were measured on samples in KBr pellets between 4000 and 400 cm^{-1} with a Perkin Elmer 1725X FTIR apparatus. UV diffuse reflection spectra were collected with a Perkin Elmer Lambda 9 spectrometer equipped with an integrating sphere, on the same KBr pellets used for the IR investigation. The Raman scattering was investigated with a Dilor XY dispersive spectrometer equipped with a Thomson 1024 CCD detector and an optical microscope. In this "micro-Raman" configuration, the volume investigated is about 1 μm^3 or less. The powder is simply scattered on a microscope slide, and the spectra are collected systematically for several grains allowing control of the homogeneity of the sample at this level. For the Raman investigations, the spectrometer was equipped with a 1800 grooves/mm grating giving a spectral resolution of 5 cm^{-1} in the visible region. The excitation source was a krypton-argon ion laser. The Eu^{3+} luminescence spectra were recorded with the same apparatus, under excitation at 488 nm/20492 cm^{-1}. This excitation level is situated above the $^5D_1$ energy level of Eu^{3+}, emissions from $^5D_1$ and from $^5D_0$ towards the ground ^7F multiplet can then be observed. For this investigation, the 600 grooves/mm grating was employed with a spectral resolution of about 30 cm^{-1} (0.6 nm). As for the Raman scattering, the luminescence spectra were measured successively on different grains.

The luminescence was also investigated with a Perkin Elmer LS50B spectrofluorimeter operating in time-resolved mode, equipped with a Hamamatsu R928 photomultiplier tube. Excitation and emission bandpasses of 10 nm were used, and the excitation spectra were corrected. The $^5D_0$ emission lifetimes were measured monitoring the emission intensity at 615 nm and averaged on at least 5 separate measurements. The program calculates an average lifetime assuming a single exponential decay. The numerical values are given within ± 10%.

Results and discussion

Characterization of the complexes inside zeolites

The theoretical formulations of the starting zeolites are Y = $Na_{51}(AlO_2)_{51}(SiO_2)_{141}$, $240H_2O$ and X = $Na_{86}(AlO_2)_{86}(SiO_2)_{106}$, $240H_2O$. The measured compositions of the starting zeolites {Na}Z (Z = X or Y), Ln-exchanged zeolites {Ln}Z (Ln = La, Eu), and corresponding samples submitted to a calcination/rehydration treatment (denoted as {Ln}ZC) are gathered in Table I. The Ln^{3+} contents in {La}Y and {Eu}Y are in good agreement with one another at $12Ln^{3+}$ ions per unit cell. In the same way, similar values are obtained for {La}X and {Eu}X , where about $26Ln^{3+}$ ions are present per unit cell. From these data, one can notice that the ion exchange capacity R% (Ln^{3+} versus initial Na^{+}) achieved in Y-zeolite is lower than in X-zeolite: R% ∼ 70% and 90% respectively. The complexes were prepared in a second step by allowing diffusion of DP ligand from a solution to the Ln^{3+} exchanged zeolites. The ligand content was determined by chemical analysis (C and N) and is reported in Table 1. About 1DP ligand for 1Eu (or 1La) ion is incorporated in {Ln}Y. In the X-zeolite, although up to $28Ln^{3+}$ per unit cell have been introduced, there are only 4 to 5 DP incorporated in the complexation process.

All the Ln-exchanged and complexed (Ln-exchanged) zeolites exhibit good quality X-ray diffraction patterns. All can be indexed with the unit cell data of the corresponding zeolite, no additional impurity peak was detected.

The formation of the Ln(DP) complexes was followed by Raman, IR and UV spectroscopies.

Our investigation of the Raman scattering was performed on the lanthanum containing samples in order to avoid ambiguities with the emission lines when europium containing samples are investigated. The strongest Raman band for {La}Z occurs in the 450–550 cm^{-1} region [13, 14]. After complexation by the DP ligand, new bands are observed at

Table 1. Results of the chemical analysis and Ln to Na exchange capacities R% [M]: number of moles of element M per unit cell calculated using [M] = $x_M \times 192/(x_{Al} + x_{Si})$ with x_M the content in moles for 1 g sample.

	[Na]	[La]	[Eu]	[Al]	[Si]	n = Si/Al	[DP] (C/N)[a]	[H_2O][b]	R%[c]	R%[d]
{Na}Y	49.1			50.7	141.3	2.71		218		
{La}Y	16	11.7		52.5	139	2.65		260	71.5	67.5
{La(DP)}Y	15.5	11.0		50.8	141.2	2.78	11.1//10.4	162		
{Eu}Y	17.9		11.9	52.7	139.3	2.64		272	72.7	63.5
{Eu(DP)}Y	17.3		11.8	52.4	139.6	2.66	12.8//11.7	200		
{Eu}YC	16.5		12.1	53.3	138.6	2.60		257		
{Eu(DP)}YC	15.4		12.3	53.4	138.6	2.60	6.0//5.5	238		
{Na}X	83.5			86.7	105.3	1.21		208		
{La}X	12.6	25.4		95.0	97.0	1.01		273	91.3	84.9
{La(DP)}X	8.3	25.3		87.9	104.0	1.18	5.6//5.1	268		
{Eu}X	2.8		27.5	90.6	101.5	1.12		291	98.8	96.5
{Eu(DP)}X	7.3		27.8	93.2	98.8	1.06	3.8//5.0	288		
{Eu}XC	8.4		24.8	84.5	107.5	1.27		239		
{Eu(DP)}XC	7.0		28.0	93.4	98.6	1.05	6.9//6.9	239		

[a] [DP](C) and [DP](N) from x_C and x_N, respectively.
[b] [H_2O] = $[(1/2)x_H \times 192/(x_{Al} + x_{Si})] - 3$[DP](C).
[c] $3[Ln] \times 100/[Na]_i$: $[Na]_i$ from {Na}Z [Ln] from {Ln}Z.
[d] $[Na]_i - [Na]_f \times 100/[Na]_f$: $[Na]_i$ from {Ln}Z.

1020, 1405, 1460 and 1590 cm^{-1}. This new set obviously pertains to the organic part of the hybrid and presents many analogies with the spectrum of [Ca(DP)]·3H_2O described and assigned in Ref. [15]. Moreover, the homogeneous distribution of the organic ligand in the zeolite matrix was confirmed by this Raman investigation.

More information on the DP to Ln bonding in the hybrids may be extracted from the IR absorption spectra (Figure 1). Strong absorption bands of the zeolite framework and of the zeolitic water are observed between 400 and 1200 cm^{-1} and 1600 and 1800 cm^{-1}, respectively. The incorporation of the organic ligand in the matrix results in the superposition of a series of narrow and weak lines. The more interesting region for investigating the Ln-DP association is from 1200 to 1800 cm^{-1}. The assignments are based upon those made by Carmona [15] on the acid and the calcium salt. The {Eu(DP)}Y spectrum shows bands between 1620 and 1590 cm^{-1} and between 1407 and 1380 cm^{-1} assignable to asymmetric and symmetric stretching vibrations of the carboxylate group, respectively. These bands are red or blue shifted with respect to the free ligand DPH_2 where ν_{as}(OCO) and ν_s(OCO) are located at 1700 and (1330, 1300) cm^{-1}. One may conclude that all the carboxylic groups COOH are transformed to carboxylates CO_2^- when the ligand is inserted into EuY. The remaining bands around 1575, 1460 and 1275 cm^{-1} may be assigned to the vibrations of the skeletal modes of the pyridine ring. These vibrations are not greatly shifted in {Eu(DP)}Y with respect to DPH_2 and are of little diagnostic value for supporting a metal-pyridine coordination. Very similar characteristics are observed for {Eu(DP)}X and {La(DP)}Z.

Finally, the diffuse reflectance (DR) spectra measured on {Ln(DP)}Z when compared to {Ln}Z exhibit a broad and strong absorption band around 275 nm. The same band is observed for [$Eu(DP)_3Na_3$]·nH_2O. This absorption may be unambiguously assigned to the $n \rightarrow \pi^*$ and $\pi \rightarrow \pi^*$ transitions of the pyridyl chromophore, which are almost completely overlapped [16].

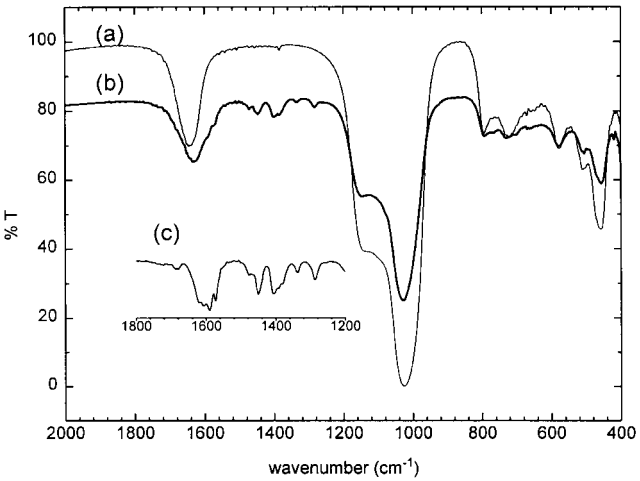

Figure 1. IR absorption spectra. (a) {Eu}Y; (b) {Eu(DP)}Y; (c) difference {Eu(DP)Y} - {Eu}Y.

Luminescence measurements

Eu-exchanged Zeolites

We will first recall some structural features of the faujasite-type zeolites X and Y. The convenient building block is the sodalite cage (or β-cage). Each sodalite cage ($\sim$ 6.6 Å diameter) is connected to four similar cages via hexagonal prisms ($\sim$ 1.8 Å diameter) forming the small pore system in the zeolite. The arrangement of the α-cages builds the so-called super cages or α-cages ($\sim$ 12.6 Å diameter) connected by large windows ($\sim$ 7.5 Å diameter), both constituting the

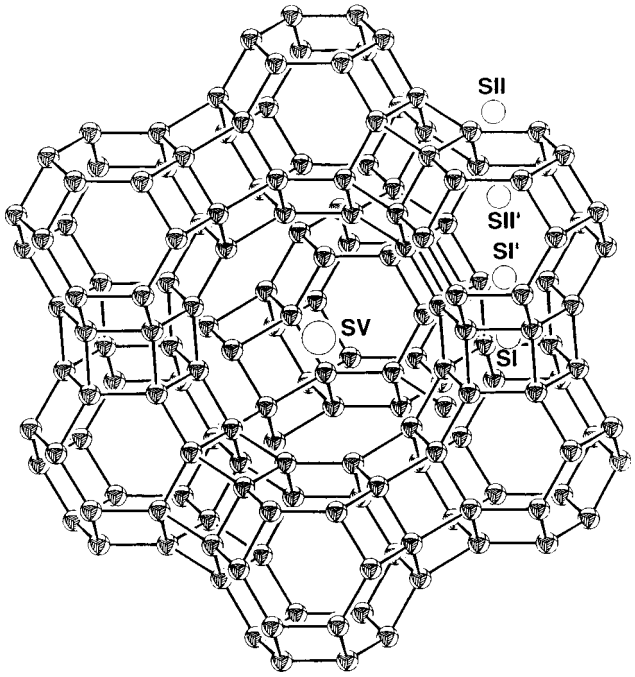

Figure 2. ORTEP representation of the faujasite structure. The T (Al or Si) framework cations and the T—T bonds are represented; the oxygen atoms are not drawn. The open circles image the non-framework Ln^{3+} sites (see text).

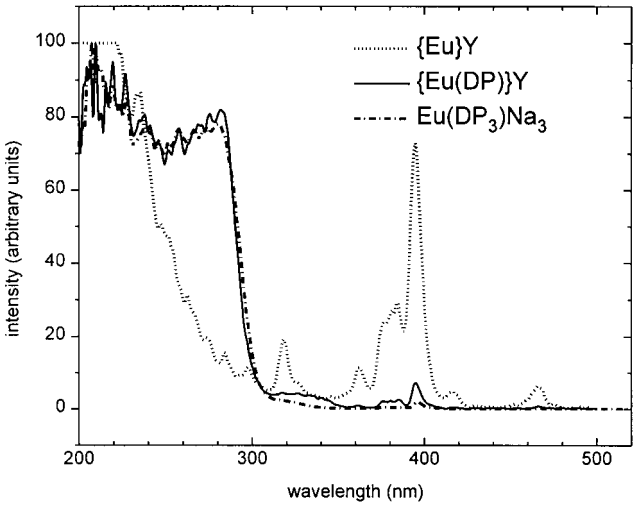

Figure 3. Examples of excitation spectra recorded on powder samples: monitoring wavelength: 615 nm.

large pore system. Several works were devoted to determine the localization of the rare earth cations at extra-framework sites [17–26] : SI (the center of the hexagonal prisms), SI′ and SII′ (inside the sodalites) SII and SV (inside the α-cages). A schematic view of the structure and of the localization of these sites is shown in Figure 2.

For {Eu}Y and {Eu}X studied hosts, excitation at 395 nm (metal-centered-absorption) gives a typical europium (III) emission containing the expected sequence of $^5D_0 \rightarrow {}^7F_J$ transitions. The $^5D_0$ lifetimes of the probed ions were determined by recording the intensity of the emitted light at the most intense $^5D_0 \rightarrow {}^7F_J$ transition, assuming that the emission decay is monoexponential. Although the Eu^{3+} in different environments will certainly give rise to different decays, we measured an average of the $^5D_0$ lifetimes of the probed ions and we were able to estimate the lifetime lengthening that parallel the various treatments imposed on the {Eu}Z. The luminescent lifetime (τ) values are gathered in Table 2. The observed deexcitation probability $1/\tau$ (obs) is enhanced by all the non radiative decay pathways: coupling to the framework vibrations, to the ligand vibrations and to the OH vibrations. The last one is the more efficient pathway because the associated vibrational energy is higher (see for instance Ref. [27]).

The $^5D_0$ lifetime in {Eu}Y (140 μs) is very similar to that measured for aqueous solutions of $EuCl_3$: 110 μs (this work), or 104 μs [28], while it is much longer (250 μs) in {Eu}X. Moreover, the lifetime is increased by a factor of 1.7 and 2.2 in {Eu}X and {Eu}Y respectively, after calcination and rehydration treatment. These data clearly suggest different hydration states of the lanthanide ion.

The Eu^{3+} luminescence excitation spectra were recorded at room temperature monitoring the $^5D_0 \rightarrow {}^7F_2$ emission at 615 nm. For the {Eu}Z samples, the intra-$4f^6$ narrow line transitions are observed between 500 and 300 nm (Figure 3). The strong and broad absorption at shorter wavelengths is assigned to the $O^{2-} \rightarrow Eu^{3+}$ charge transfer transition, and to matrix absorption.

Some of the Eu^{3+} luminescence spectra recorded at high resolution on the {Eu}Z and {Eu}ZC samples are displayed in Figure 4. The spectra exhibit broad and partly unresolved $^5D_0 \rightarrow {}^7F_J$ emission bands (as well as $^5D_1 \rightarrow {}^7F_J$ for {Eu}Y). The emission spectrum recorded for one sample is in fact the sum of several individual spectra if there are several types of Eu^{3+} surroundings in the sample. The spectrum observed for {Eu}Y is very peculiar because the intensity ratio $^5D_0 \rightarrow {}^7F_2/{}^5D_0 \rightarrow {}^7F_1$ is about 0.4 instead of 2 for the other samples. This spectrum is actually very similar to that of the completely hydrated Eu^{3+} as observed in europium chloride solution, confirming the lifetime results. These features are not observed for {Eu}X. After having been calcined then rehydrated, the {Eu}YC and {Eu}XC samples exhibit more complex emission spectra, the emission lines superimposed on a broader background.

These results call for some comments. The exchange capacity measured in the present work is 70% in Y (*vide supra*), and we observed that most Eu^{3+} remains fully hydrated. These observations are in agreement with earlier works where it was shown that Na^+ in the small pore system of the Y-zeolite are not exchanged by Ln^{3+} in a single exchange. As for the location of the rare earth ions in hydrated Y- or faujasite, all authors agree with the existence of hydrated Ln^{3+} in the supercages at SV. The remaining ions are found in the supercages at another undefined position [18], at SII [24] or in the sodalites at SI′ [19]: in these last two locations, Ln^{3+} are partly dehydrated and bound to framework oxygens. These differences illustrate the difficulty of comparing hydrated zeolite samples from different origins. For instance, Lee *et al.* [29] in their investigation by time resolved Eu luminescence did not observe the spectrum of

Table 2. Estimation of the DP → Eu transfer efficiencies W_{DP-Eu},[a] and $^5D_0$ emission decay times τ.

	I_{275} [b]	I_{395} [b]	[DP][c]	[Eu][c]	W_{DP-Eu} [a]	τ $^5D_0$ (ms)
{Eu}Y	–	–	–	–	–	0.14 ± 0.01
{Eu(DP)}Y	80	7.2	12	12	0.9	0.26 ± 0.02
{Eu}YC	–	–	–	–	–	0.31 ± 0.03
{Eu(DP)}YC	60	2.7	5.7	12	8.2	0.25 ± 0.02
{Eu}X	–	–	–	–	–	0.25 ± 0.02
{Eu(DP)}X	95	6	4.5	28	21.9	0.65 ± 0.06
{Eu}XC	–	–	–	–	–	0.42 ± 0.04
{EU(DP)}XC	80	3	7	28	15.2	0.42 ± 0.04
$[Eu(DP)_3Na_3]\cdot nH_2O$	76	2	3	1	12.7	1.50 ± 0.13
1Eu–3DP[d]	47	0.3	3	1	52.2	1.57 ± 0.16
$Eu^{3+}(H_2O)_{8.9}$ [c]	–	–	–	–	–	0.11 ± 0.01

[a] $W_{DP-Eu} = I_{275}[Eu]/I_{395}[DP]^2$ for the {Eu(DP)}Z samples and $= I_{275}[Eu]/I_{395}[DP]$ for the reference samples (see text).
[b] I_{275} and I_{395} in arbitrary units from the luminescence excitation spectra.
[c] [Eu] and [DP] from Table I.
[d] Excitation spectrum in (1Eu-3DP) 4×10^{-5} M in diluted NaOH, pH = 6.5, lifetime in (1Eu-3DP) 2×10^{-2} M in diluted NaOH, pH = 6.9.
[e] ($EuCl_3$) 10^{-1} M in H_2O.

hydrated europium in {Eu}Y, but they recorded a spectrum more analogous to the one we obtained on {Eu}X. In contrast to the Y-zeolite, the ion exchange by Ln^{3+} in {Na}X is almost complete in a single step (about 90%). Luminescence lifetimes and emission spectra show that the europium ions are on average less surrounded by H_2O or OH vibrators and thus are bonded in part to zeolite framework oxygens. Part of the trivalent cations enters the sodalite [18, 20]. Literature data indicate that most of the ions are distributed at SII and SI' sites, a small proportion is at SV [18]. Our luminescence results represent on average this localization of Eu^{3+} at less hydrated, more tightly bonded sites in X than in Y.

In {Eu}XC and {Eu}YC samples, the europium ions are distributed over several sites, and the distribution is different depending on the nature of the zeolite. This is supported by the observed systematic increase in the Eu^{3+} emitting lifetime, reflecting the lowering of linked OH vibrators, and by the major modifications exhibited by the emission spectra upon calcination. As a matter of fact, although some minor discrepancies still persist between the conclusions of Refs [17, 18, 20–26], it is well established that upon calcination of {Ln}Z, the Ln^{3+} ions migrate to the sodalite cages (SI′), and at higher temperature to the hexagonal prisms (SI). It is worthy of note that the lanthanides remain in the sodalites or the hexagonal prisms upon rehydration.

Eu(DP) complexes

Several previous studies were related to the spectroscopy of europium-dipicolinato complexes [12, 27, 28, 30, 31]. The results obtained on solutions from the different sources are more coherent. Calculations have shown [30] that above pH = 6, complexation is fairly complete for 1Eu–3DP solutions. The $[Eu(DP_3)]^{3-}$ (1 : 3) species is formed, in which each (DP) ligand coordinates by an oxygen of each carboxylate group and by the nitrogen of the pyridine ring to the central ion. In this species there is no water molecule in the first coordination sphere, the symmetry at the europium ion is close to D_{3h}. The different measurements conclude coherently that the $^5D_0$ emission lifetime is 1.60 ± 0.05 ms. The lifetime in the 1 : 1 and 1 : 2 species are 0.169 and 0.304 ms respectively [28]. Although the same $[Eu(DP_3)]^{3-}$ species exists in several crystalline solids, the reported lifetimes are quite different: 2.02 ms in $[N(C_2H_5)_4]_3[Eu(DP)_3]\cdot nH_2O$ at 77 K [12] and 1.30 ms in $Na_3[Eu(DP)_3]\cdot 15H_2O$ at 300 K [27]. Here, we obtained τ = 1.50 ms for $[Eu(DP)_3Na_3]\cdot nH_2O$.

The energy transfer from the pyridyl unit to bound Eu^{3+} is proved by the occurrence of the absorption band at 275 nm in the luminescence excitation spectra (an example is shown in Figure 3 for $[Eu(DP)_3Na_3]\cdot nH_2O$).

Eu(DP) complexes encapsulated in zeolites

The $^5D_0$ emitting lifetimes exhibit a pronounced increase in hydrated X and Y zeolites upon complexation by the DP ligand, but there is no increase upon complexation in the calcined matrices (Table 2). The average lifetime measured in the {Eu(DP)}Z never reaches the values (1.3–2.02 ms) measured in the reference compounds.

The excitation spectra (Figure 3) in the {Eu(DP)}Z samples unambiguously prove that the ligand to lanthanide complexation has been achieved to some extent within the matrices. This complexation is further evidenced by the modifications occurring in the Eu^{3+} emission spectra after addition of the ligand. The modification is particularly spectacular in {Eu(DP)}Y versus {Eu}Y because the $^5D_0 \rightarrow {}^7F_2/{}^5D_0 \rightarrow {}^7F_1$ ratio is inverted. Although less important, some differences may also be observed in the $^5D_0 \rightarrow {}^7F_2$ region. In the calcined zeolites, the introduction of the ligand also causes modifications of the emission spectra; more clearly visible because the lines are slightly better resolved than in the calcined hosts (Figure 4).

It seems useful to compare the efficiencies of the DP to Eu energy transfer W_{DP-Eu} after encapsulation and in the

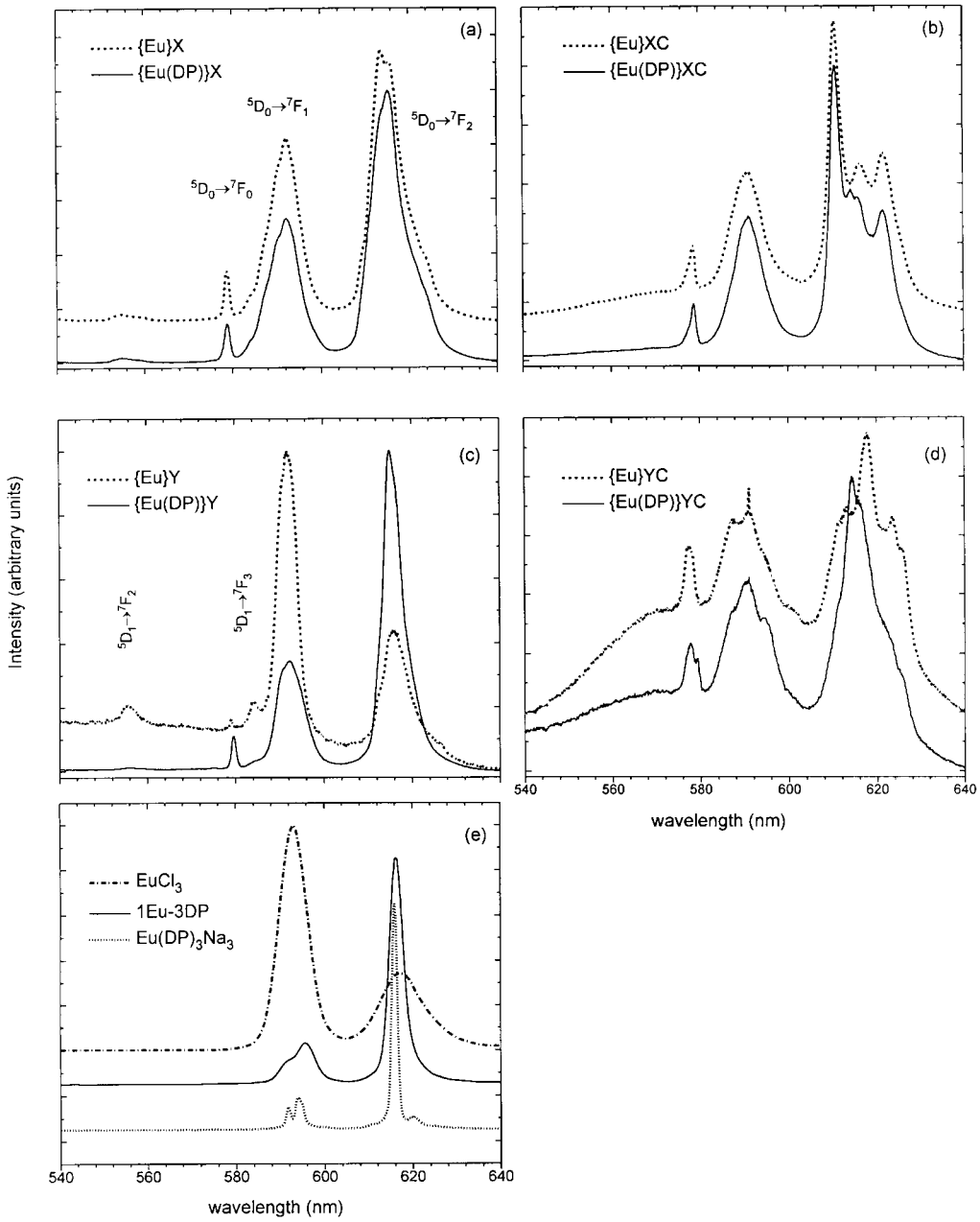

Figure 4. (a-d) Emission spectra recorded on {Eu}Z samples before and after complexation by the DP ligand with the micro-raman setup, excitation wavelength: 488 nm. (e) Emission spectra of solutions 1Eu-3DP: 2×10^{-2} M in diluted NaOH, and $EuCl_3$: 10^{-1} M in water, recorded with the low-resolution spectrofluorimeter, excitation wavelengths: 275 and 395 nm, respectively; emission spectrum of $Eu(DP)_3Na_3 \cdot nH_2O$ with the micro-Raman setup, excitation wavelength: 488 nm.

reference samples. We define W_{DP-Eu} as the ratio of the europium excitation intensity via DP absorption and energy transfer (at 275 nm) over the direct intra-4f^n $^7F_0 \rightarrow {}^5L_6$ excitation intensity at 395 nm: $W_{DP-Eu} = I_{275}/I_{395}$ (Equation (1)). This estimation must be done for one Eu–DP pair, the problem here is to consider adequate concentrations of the species because one only knows the overall concentrations in the composites (Table 1) and all Eu^{3+} ions in the sample absorb at 395 nm. The number of europium ions linked to at least one ligand cannot exceed [DP]; this limiting value is taken for the estimation, the extra europiums being linked to the zeolite framework only. In the first approximation, the intra-4f^n $^7F_0 \rightarrow {}^5L_6$ absorption intensity is the same for all Eu^{3+}, whatever their environments, and the denominator in Equation (1) is given by $I_{395} \times ([DP]/[Eu])$. The numerator is $I_{275}/[DP]$. For the reference samples, all containing $[Eu(DP)_3]^{3-}$, the number of associated Eu is set equal to 1 for 3DP so that the equation becomes $W_{DP-Eu} = I_{275}/3I_{395}$. The calculated W_{DP-Eu} are gathered in Table 2. Actually, it has been measured in Ref. [30] that the $^7F_0 \rightarrow {}^5L_6$ absorption intensity varies by a factor 2 in the Eu–nDP solutions, but the differences observed here on the W_{DP-Eu} parameters are widely more important than the error relative to this variation. The W_{DP-Eu} parameter increases about 25 times going from {Eu(DP)}Y to {Eu(DP)}X. The DP to Eu energy transfer is more efficient when the complex [Eu–

$DP]^+$ is more tightly bonded to framework oxygens (the case of {Eu(DP)}X) than when it is bonded to water molecules (the case of {Eu(DP)}Y). It is worth noting that this energy transfer efficiency is even higher in {Eu(DP)}X than in the complex $[Eu(DP)_3]^{3-}$ in the solid state.

Having in mind the interpretations of diffraction data in the works mentioned above, and considering the results of our investigation, we may suggest a model for the incorporation of DP in the different zeolites studied here. About 1DP for 1Eu (or 1La) is incorporated in {Ln}Y. The $Eu^{3+}(H_2O)_{8-9}$ species in the supercage are replaced on average by $[Eu(DP)]^+$ $(H_2O)_{5-6}$. The $^5D_0$ average lifetime goes from 140 to 260 μs: longer but not very different from the values for the same species in solution (113 and 169 μs respectively). In the X zeolite, although up to 28 Eu^{3+} per unit cell (u. c.) have been introduced, there are only 4 to 5 DP incorporated in the complexation process (similar values are found for {La}X). The Ln^{3+} located at SII in the super-cages are linked simultaneously to framework and to ligands. Considering the results in Ref. [18], 12La per u.c. would be in site II whereas only 4–5 DP are incorporated. The $^5D_0$ average lifetime also noticeably increases during this process (250–650 μs). The agreement with the structural determinations is less straightforward for the calcined hosts. Upon calcination the Eu^{3+} ions tend to migrate into the small pore system. On the other hand, the "dimension" of a DP ligand may be estimated from CPK model to be $\sim$7 Å, the DP can therefore hardly migrate in the small pore system and are retained in the supercages. Six and seven DP per u.c. were incorporated in {Eu(DP)}YC and in {Eu(DP)}XC, respectively. The emission spectra of the {Eu(DP)}Z are more complex than for the un-calcined samples, several individual spectra obviously overlap in the resulting emission (Figure 4). The $^5D_0$ average lifetimes exhibit no more change after complexation, but the excitation energy transfer occurs with a high efficiency in these hosts, evidencing the complexation. Then one may conclude that the Eu^{3+} migration was not complete and that some Eu^{3+} ions remained in the supercages, at SII sites.

Conclusion

Rare earth (Ln^{3+} = La^{3+} or Eu^{3+}) complexes with the dipicolinato-($C_5H_3N(COO^-)_2$ = DP) ligand were synthesized inside the super-cages of two zeolite matrices X and Y. The degree of complexation never exceeds 1DP/1Ln; moreover not all the Ln but only those which are in the super-cages may be complexed. The europium-containing complexes exhibit a strong $^5D_0 \rightarrow {}^7F_J$ luminescence under excitation at 275 nm in the absorption band of the ligand, evidencing the DP to Eu energy transfer. The efficiency of the transfer, estimated from the relative intensity of the DP excitation band, depends on the localisation of the complex with respect to the alumino-silicate framework. We observe that it is more efficient when the complexed europium $[Eu(DP)]^+$ is directly bonded to the framework oxygen atoms rather than to residual water molecules, but that the number of such tightly bonded complexes was always smaller than one (0.6–0.9) per super-cage in our synthesis conditions. On the other hand, when all the europium ions are involved in fully hydrated $Eu^{3+}(H_2O)_{8-9}$ in the super-cages, the case of {Eu}Y zeolite, up to 1.5 $[Eu(DP)]^+$ per cage could be synthesized; in this last case the transfer is nevertheless less efficient.

Acknowledgements

The authors wish to thank Drs A. Gourdon and J. C. Trombe (CEMES) for critical discussions and Mrs R. Enjalbert (CEMES) for her help in handling the ORTEP program.

References

1. N. Herron: *CHEMTEC* 542 (1989).
2. B. V. Romanovsky and A. G. Gabrielov: *J. Mol. Catal.* **74**, 293 (1992).
3. R. F. Parton, I. F. G. Vankelecom, M. J. Casselman, C. P. Bezoukhanova, J. B. Uytterhoven, and P. A. Jacobs: *Nature* **370**, 541 (1994).
4. C. A. Bessel and D. R. Rolison: *J. Phys. Chem. B* **101**, 1148 (1997).
5. W. H. Quayle and J. H. Lunsford: *Inorg. Chem.* **21**, 97 (1982).
6. K. J. Balkus Jr. and J. Shi: *Micropor. Mater.* **11**, 325 (1997).
7. Y. Zhang, M. Wang, and J. Xu: *Mater. Sci. Eng. B* **47**, 23 (1997).
8. A. C. Franville, D. Zambon, R. Mahiou, S. Chou, Y. Troin, and J. C. Cousseins: *J. Alloys Compd.* **275–277**, 831 (1998).
9. I. L. Rosa, O. A. Serra, and E. J. Nassar: *J. Lum.* **72–74**, 532 (1997).
10. M. Alvaro, V. Fornes, S. Garcia, H. Garcia, and J. C. Scaiano: *J. Phys. Chem. B* **102**, 8744 (1998).
11. M. Hilder, U. Kynast, C. Lau, and K. Schulte: "Lumineszierende Eu- und Tb- complexes in zeolith X", poster, DFG – kolloquium "nanoporose Kristalle", Bonn (1999).
12. P. A. Brayshaw, J. C. G. Bunzli, P. Froidevaux, J. M. Harrowfield, Y. Kim, and A. N. Sobolev: *Inorg. Chem.* **34**, 2068 (1995).
13. P. K. Dutta and J. Twu: *J. Phys. Chem.* **95**, 2498 (1991).
14. C. Brémard and M. Le Maire: *J. Phys. Chem.* **97**, 9695 (1993).
15. P. Carmona: *Spectrochim. Acta* **36A**, 705 (1980).
16. G. Coppens, C. Gillet, J. Nasielki, and E. VanderDonckt: *Spectrochim. Acta* **18**, 1441 (1962).
17. J. V. Smith, J. M. Bennett, and E. M. Flaningen: *Nature* **215**, 241 (1967).
18. D. H. Olson, G. T. Kokotailo, and J. F. Charnell: *J. Colloid Interface Sci.* **28**, 305 (1968).
19. J. M. Bennett and J. V. Smith: *Mater. Res. Bull.* **4**, 343 (1969).
20. J. M. Bennett, J. V. Smith, and C. L. Angell: *Mater. Res. Bull.* **4**, 77 (1969).
21. A. K. Cheetham, M. M. Eddy, and J. M. Thomas: *J. Chem. Soc., Chem. Commun.* 1337 (1984).
22. K. J. Chao and J. Y. Chern: *J. Phys. Chem.* **93**, 1401 (1989).
23. D. R. Shy, S. H. Chen, J. Lievens, S. B. Liu, and K.-J. Chao: *J. Chem. Soc. Faraday Trans.* **87**, 2855 (1991).
24. H. Klein, H. Fuess, and M. Hunger: *J. Chem. Soc. Faraday Trans.* **91**, 1813 (1995).
25. K. Gaare and D. Akporiaye: *J. Phys. Chem. B* **101**, 48 (1997).
26. J. G. Nery, Y. P. Mascarenhas, T. J. Bonagamba, and E. F. Souza-Aguiar: *Zeolites* **18**, 44 (1997).
27. W. deW. Horrocks Jr. and D. R. Sudnick: *J. Am. Chem. Soc.* **101**, 334 (1979).
28. W. deW. Horrocks Jr. and D. R. Sudnick: *Acc. Chem. Res.* **14**, 384 (1981).
29. S. Lee, H. Hwang, P. Kim, and D.-J. Jang: *Catal. Lett.* **57**, 221 (1999).
30. K. Binnemans, K. Van Herck, and C. Görller-Walrand: *Chem. Phys. Lett.* **266**, 297 (1997).
31. G. M. Murray , R. V. Sarrio, and J. R. Peterson: *Inorg. Chim. Acta* **176**, 233 (1990).